Soft Matter

ARTICLE TYPE

Supplementary Informations for: Conformation and dynamics of partially active linear polymers

Marin Vatin,[*a,b] Sumanta Kundu,[a,b,c] and Emanuele Locatelli[a,b]

1 Number of arrangements of the active monomers: theoretical calculation

We report here on the theoretical estimate of the number of possible arrangements of the active monomers as a function of the their fraction p. We recall that we considered four different settings in the main text: a) the active monomers are distributed at random along the chain, b) the active monomers are arranged in one active block, c) the active monomers are arranged in two, non-overlapping active blocks, d) the active monomers are arranged in three, non-overlapping active blocks. We will provide here estimates for settings a)-c).

The number of possible arrangements of $N \cdot p$ active monomers within a total of N monomers can be calculated using combinatorial methods. In the random case, the number of configurations $\mathcal{N}$ is simply given by the binomial coefficient:

$$\mathcal{N} = \frac{N!}{(N \cdot (1-p))! \cdot (N \cdot p)!} \tag{S1}$$

where both $N \cdot p$ and $N \cdot (1-p)$ are integers or should be rounded to the closest integer. The set of arrangements where the active monomers are organized in a single block of $N \cdot p$ monomers is a subset of the random case; the number of configurations is simply given by:

$$\mathcal{N}_1(N,p) = N \cdot (1-p-1/N) \underset{N \gg 1}{\sim} N \cdot (1-p) \tag{S2}$$

where $N \cdot (1-p)$ is the number of inactive monomers; the additional $1/N$ accounts for fact that the first monomer is always passive. The approximation is valid in the limit of very large chains. Finally, in the case of two identical blocks, totalling $N \cdot p$ active monomers, the number of arrangements can be approximated as

$$\mathcal{N}_2 = \frac{\mathcal{N}_1(N \cdot p/2, p/2) \cdot \mathcal{N}_1(N \cdot (1-p)/2, p/2)}{2} \tag{S3}$$

where the factor $1/2$ accounts for the fact that the order of the blocks does not matter. Note, however, that the formula is based on the approximation that the blocks are independent, i.e. all positions are possible and may overlap. This approximation remains reasonable as long as the percentage of active monomers

Dipartimento di Fisica e Astronomia, Università di Padova, via Marzolo 8, I-35131 Padova, Italy. [b] INFN, Sezione di Padova, via Marzolo 8, I-35131 Padova, Italy. [c] International School for Advanced Studies (SISSA), 34136, Trieste, Italy.

remains low and, in any case, overestimates the total number of arrangements. The theoretical predictions are shown in Fig. S1.
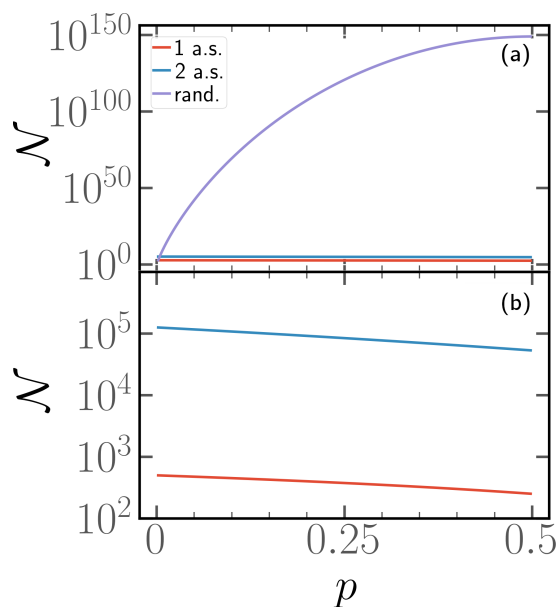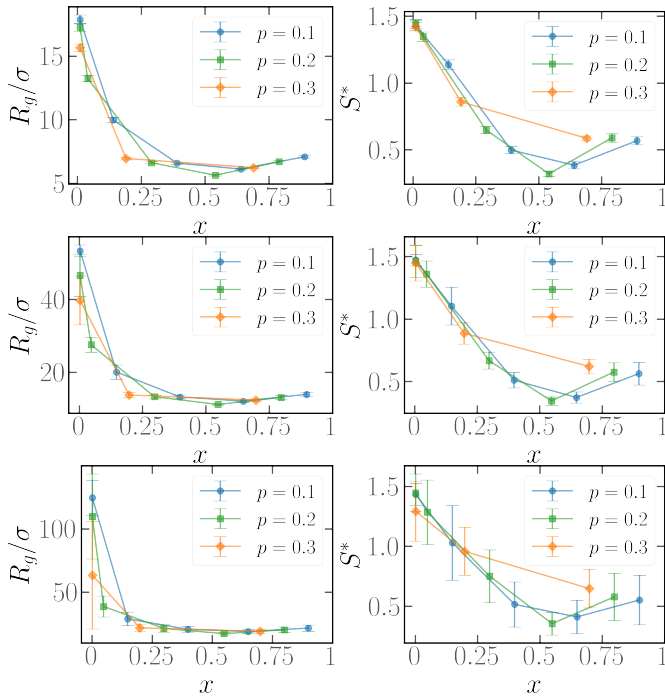

Fig. S1 Number of arrangements $\mathcal{N}$ of $N \cdot p$ active monomers (with $N = 500$) along the polymer chain as a function of the percentage of active monomers p.

As shown, the number of arrangements is overwhelmingly larger in the random case than in the one block or two blocks cases. Thus, albeit blocks are possible random arrangements, they are so rare that their effect is negligible at the population level.

2 Gyration radius, asphericity and prolateness

In this section, we report complementary data on the size and shape of polymer chains: we report data for polymers of different contour length and Péclet number with respect to the main text.

In Fig. S2, we report the mean gyration radius and prolateness as a function of the parameter x for chains of different degree of polymerization $N = 100, 300, 600$. We can observe that the features, reported in the main text for $N = 500$, are visible here as well. Here, no smoothing has been applied to the data; error bars refer to the standard error of the mean over $M = 25$ independent identical realizations. This confirms that the general features reported in the main text remain valid for polymers of different length, bearing in mind that, for the values of p and x highlighted

Fig. S2 Mean Gyration Radius (left), and prolateness (right) as a function of the parameter x for Pe $=10$, different values of p and $N = 100$, $N = 300$ $N = 600$.

in the main text, the scaling breaks due to self-entanglements.

In Fig. S3 we show the mean gyration radius, asphericity and prolateness as a function of the parameter x for chains of length $N =500$ at fixed Pe $=0.1$ and different values of p. We thus check whether the contour position of the active section influences the conformation and the shape of the chain even at low activity. Indeed, we find that the values of the shape parameters are in semi-qualitative agreement with the values reported in the main text at Pe $=10$. This means that, even if the individual monomers have a low activity, the effects of the activity on the conformation of the chain can be relevant. Indeed, the expected value of R_g, at $Pe =0$, is $R_g/\sigma \approx 0.59 \cdot N^{0.588} = 20.21$ (for the Kremer-Grest model, we take the scaling prediction from the Supplemental Material of ref. [1]); thus R_g increases almost by a factor of two at $x = 1/N$ and shrinks by roughly 30% at $x = (1-p)/2$. On the contrary, for a fully active polymer, the relative difference is, at Pe $=0.1$, of the order of a few percent. However, as suggested by the small values of the non-Gaussian parameter reported in the main text, the effect of the contour position of the active block on the polymer dynamics at small values of Pe is not equally relevant.

3 End-to-end autocorrelation function

In this section, we report complementary data on the time correlation function of the end-to-end vector of the active section at fixed Pe $=10$.

In Fig. S4 we report the time correlation function of the end-to-end vector of the active section as a function of the rescaled time tD_0/σ^2 at fixed $N =100$ and Pe $=10$ for different values of x. We show in panel (a) data referring to $p = 0.1$ and in panel (b) data referring to $p = 0.3$. We highlight that the anomalous
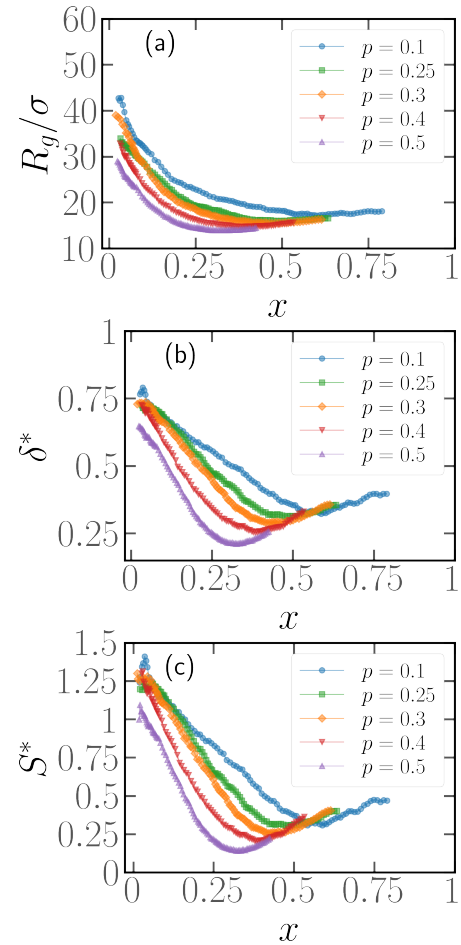

Fig. S3 (a) Gyration Radius, (b) asphericity and (c) prolateness as a function of x, at fixed Pe $=0.1$ for different values of p.

behaviour of the time correlation function is much more evident in panel (a) than in panel (b) or in the data shown in the main text. For $N =100$, $p =0.1$ the active section takes much longer time to decorrelate, to the point that its value only approaches zero at the end of the available simulation window. The tail of the correlation function looks, in the semi-log representation of the plot, almost linear; this would suggest a very slow logarithmic decay. As mentioned in the main text, this is a consequence of the effective persistence length, connected to the tangential activity.

In Fig. S5 we report the time correlation function of the end-to-end vector of the active section as a function of the rescaled time tD_0/σ^2 at fixed $N =300$ and Pe $=10$ for different values of x. We show in panel (a) data referring to $p = 0.1$ and in panel (b) data referring to $p = 0.3$. Comparing to the previous figure, we notice that that the anomalous behaviour of the time correlation function at $x = 1/N$ is less extreme for $N =300$, again simply because the length of the active block increases upon increasing N at the same value of p. As in the main text, we notice in both Figs. S4, S5 the characteristic time, associated with "tumbling" motion, increases upon increasing both N and p.

4 Bond length distribution

In this section, we report complementary data on the distribution

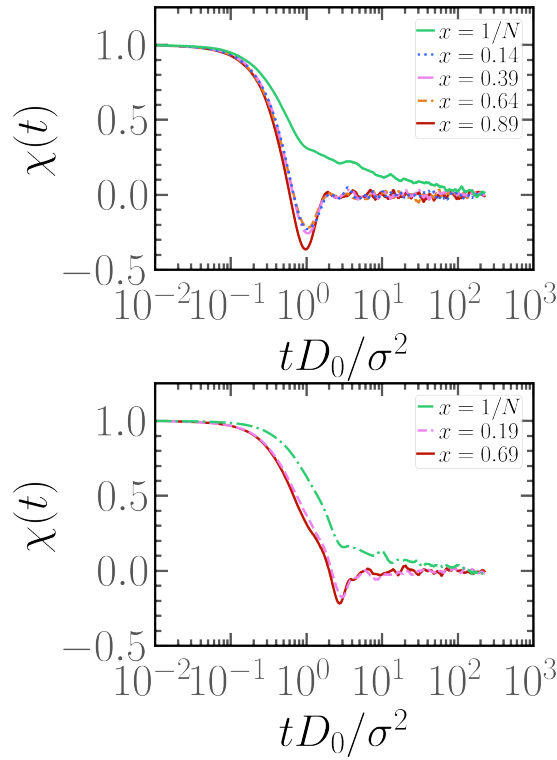Fig. S4 Time correlation function of the end-to-end vector of the active section at fixed Pe =10, $N = 100$ for different values of x and (a) $p = 0.1$ (b), $p =0.3$.

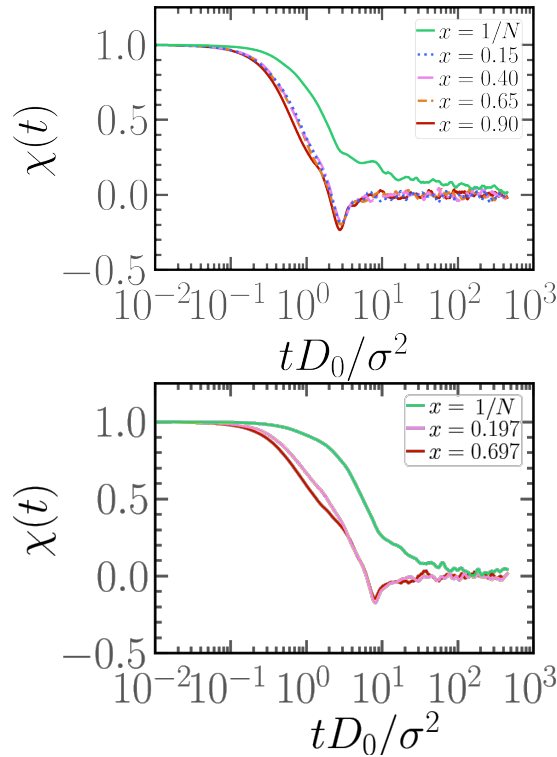
Fig. S5 Time correlation function of the end-to-end vector of the active section at fixed Pe =10, $N = 100$ for different values of x and (a) $p = 0.1$ (b), $p =0.3$.

of the distance between two consecutive monomers within the active section for $N = 500$, $p = 0.5$ and different values of Pe = 0.1, 1, 10; there is only one active block. We report the distribu-
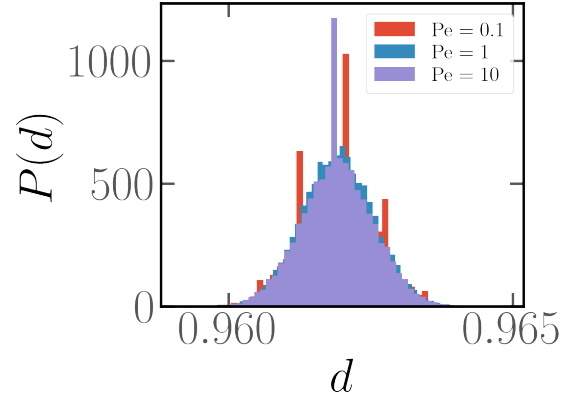

Fig. S6 Probability distribution function of the distance between two consecutive monomers within the active section at fixed for $N = 500$, $p = 0.5$ and Pe = 0.1 (red), Pe = 1 (blue), Pe = 10 (purple).

tions, sampled within the steady state, in Fig. S6. The shape of the distribution is similar for all values of the Péclet number considered in this work, suggesting that self-propulsion does not influence the bond length distribution in our model of tangentially propelled polymers, at least within the range of values considered.

5 Comparison between "model 1" and "model 2"

In this section, we present additional information concerning the comparison between the two models, "model 1" and "model 2", presented in the main text. We show that the difference between these two models manifests when the head monomer becomes active and, at the same time, when only a few monomers are active. Specifically, we discuss the properties of the end-to-end vector of the active section $\vec{R}_e^a$, i.e. the time correlation function and the distribution of its magnitude R_e^a for "model 1" and "model 2" at fixed Pe =10, $N = 100$. We further fix $x = 1/N$, such that the head monomer is active in "model 2", and we consider only small values of p.

In Fig. S7 we report the time correlation function of the end-to-end vector of the active section as a function of the rescaled time tD_0/σ^2 at fixed $N =100$ and Pe =10 for $x = 1/N$ and different values of p. We show in panel (a) data referring to "model 1" and in panel (b) data referring to "model 2". We highlight that the decorrelation time of the end-to-end vector of the active section is similar for all values of p in "model 1", while it strongly varies with p in "model 2". We observe, moreover, a non-monotonic behaviour of the decorrelation time with p in "model 2" with a maximum at $p = 0.04$. The minimum decorrelation time is obtained for $p = 0.2$ and corresponds to the one obtained for "model 1". This suggests that the difference between the two models is only relevant for small values of p or, as discussed in the main text, when the number of active monomers is smaller or equal to the activity-induced persistence length.

In Fig. S8 we report the distribution of the end-to-end distance of the active section at fixed Pe =10, $N = 100$ for different val-
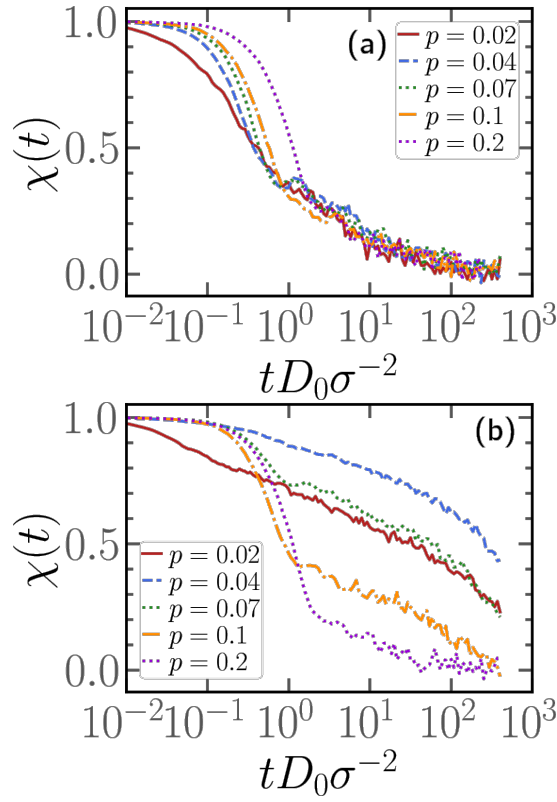
Fig. S7 Time correlation function of the end-to-end vector of the active section at fixed Pe =10, $N = 100$ for different values of x and p for model 1, when last monomer of the chain is not active (a) and for "model 2", when last monomer of the chain is active (b).
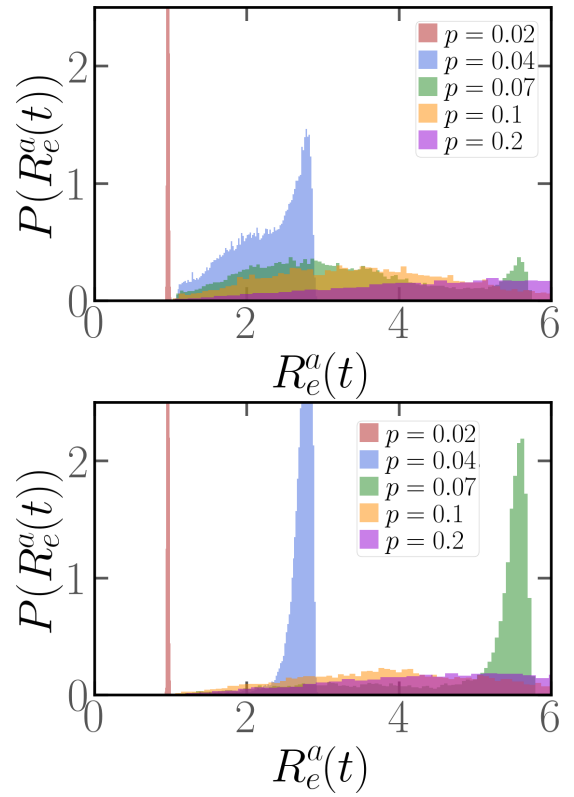

Fig. S8 Distribution of the end-to-end distance of the active section at fixed Pe =10, $N = 100$ for different values of x and p for (a) "model 1", in which the head of the polymer is not active and (b) for "model 2", in which the head of the polymer is self-propelled, with a force $f_a/3$.

ues of x and p for "model 1" (panel (a)) and "model 2" (panel (b)). We observe that, for $p \leq 0.1$, the distributions of the end-to-end distance are quite spread for "model 1", while they are much more peaked for "model 2"; in particular, the maximum value corresponds to the largest possible value $R_e^a \sim N \cdot p$. This shows that the presence of an active monomer at the end of the chain tends to straighten the active block and that such a straight section is stable. This difference practically disappears for $p > 0.1$. This observation further strengthens the conclusion drawn previously: the difference between the two models is only relevant for small values of p. Further, we remark that the large correlation times observed in Fig. S7 for "model 2" are connected to the straightening of the active block.

6 Stochastic model for the estimation of the diffusion coefficient

In this section, we propose to use the stochastic model derived in [2,3] to estimate the diffusion coefficient of the active section of the chain. Briefly, the model considers the centre of mass of the chain as subject to two stochastic forces, one due to the thermal bath $\vec{\eta}$ and one due to the self-propulsive forces $\vec{\xi} \equiv \vec{F}_a = \sum_i f_i^a$. Both terms have zero average; the thermal noise $\vec{\eta}$ obeys the fluctuation-dissipation relation

$$\langle \vec{\eta}(t)\vec{\eta}(t') \rangle = 2d \frac{(k_B T)^2}{D_0} N \delta(t - t') \tag{S4}$$

while $\vec{\xi}$ is, as a first approximation, exponentially correlated

$$\langle \vec{\xi}(t)\vec{\xi}(t') \rangle = 2d \frac{\xi_0^2}{C_t} \exp\left(-\frac{|t - t'|}{C_t}\right). \tag{S5}$$

In Eqs. (S4), (S5), d refers to the dimensionality of the system, $k_B T = 1/\beta$ is the thermal energy, D_0 is the diffusion coefficient of a single monomer, N is the degree of polymerization, ξ_0 is related to the typical amplitude of the active noise and C_t is the correlation time. The mean square displacement can be written at long times, assuming that ξ and η are not correlated, as

$$\langle r_{cm}^2(t) \rangle = \frac{(\beta D_0)^2}{N^2} 4d\xi_0^2 t + 2d \frac{(\beta D_0)^2}{N^2} \frac{(k_B T)^2}{D_0} Nt$$

$$= 2\text{Pe}^2 \frac{\langle R_e^2 \rangle}{\sigma^2} \frac{C_t D_0}{\sigma^2} \frac{D_0}{N^2} t + 2d \frac{D_0}{N} t \tag{S6}$$

where σ is the monomer diameter; we used the approximation $\vec{F}_a = f_a \vec{R}_e/\sigma^2$, $\vec{R}_e$ being the end-to-end vector, and the definition of Pe. Thus, the diffusion coefficient of the centre of mass is:

$$D = \frac{D_0}{N} + \frac{\text{Pe}^2}{d} \frac{\langle R_e^2 \rangle}{N^2\sigma^2} \frac{C_t D_0}{\sigma^2} D_0 = \frac{D_0}{N} + \frac{f_a^2 \langle R_e^2 \rangle C_t}{3N^2\gamma^2\sigma^2} \tag{S7}$$

where γ is the friction coefficient. The second expression is the same reported in [3]. For a partially active polymer, we replace $\langle R_e^2 \rangle$ with $\langle (R_e^a)^2 \rangle$, i.e. the average end-to-end distance of the active block, C_t with C_t^a, i.e. the decorrelation time of the end-to-end

vector of the active block and, in the active term, N with N_a. This latter substitution comes from the fact that the active noise $\vec{\xi}$ is generated by N_a monomers. The formula thus becomes

$$D = \frac{D_0}{N} + \frac{\text{Pe}^2}{d} \frac{\langle (R_e^a)^2 \rangle}{N_a^2 \sigma^2} \frac{C_t^a D_0}{\sigma^2} D_0 = \frac{D_0}{N} + \frac{f_a^2 \langle (R_e^a)^2 \rangle C_t^a}{3 N_a^2 \gamma^2 \sigma^2} \quad \text{(S8)}$$

We first report $\langle R_e^a \rangle = \sqrt{\langle (R_e^a)^2 \rangle}$ and C_t^a as measured from simulations. Data refer to simulations of "model 1".
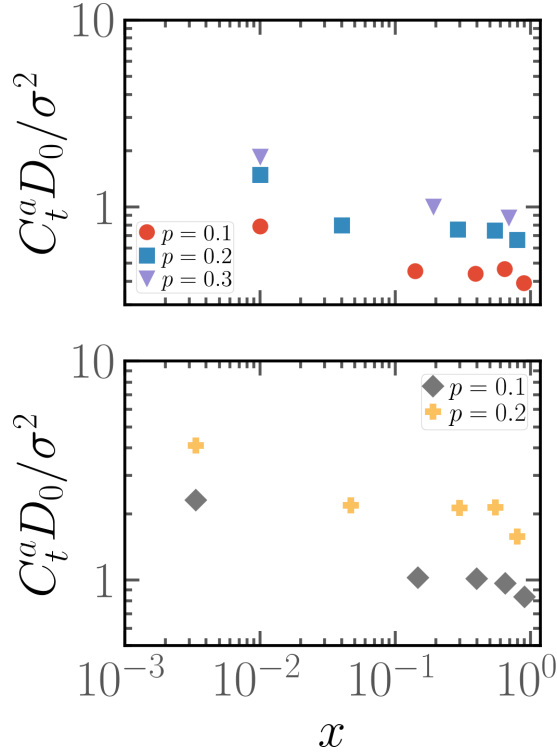

Fig. S9 Decorrelation time of the end-to-end vector of the active section as a function of x for Pe=10, $N = 100$ (a) and $N = 300$ (b) for different values of p.

Figure S9 shows the decorrelation time of the end-to-end vector of the active section as a function of x for Pe=10, $N = 100$ (a) and $N = 300$ (b) for different values of p. The decorrelation times are estimated as the times for which the autocorrelation function of the end-to-end vector of the active section is equal to $1/e$. We observe that the correlation times decrease with x and, as expected, increase with p and N, simply because the size N_a of the active section increases upon increasing N or p. Next, in Fig. S10 we report the end-to-end distance of the active section as a function of x for Pe=10, $N = 100$ (a), $N = 300$ (b) and $N = 600$ (c) for different values of p. We observe for $\langle R_e^a \rangle$ a trend similar to the one observed for C_t^a: the end-to-end distance of the active section decreases with x and increases with p and N. However, for $x \gtrsim 0.1$, $\langle R_e^a \rangle$ remains markedly constant. These data suggest that, unless the active block is right at the head of the chain, the globule-like character of the active block is not affected by the position of said block along the chain.

The two quantities just reported, $\langle R_e^a \rangle$ and C_t^a, allow to estimate the long time diffusion coefficient using Eq. S8. The diffusion coefficient thus obtained is reported in Fig. S11 as a function of x
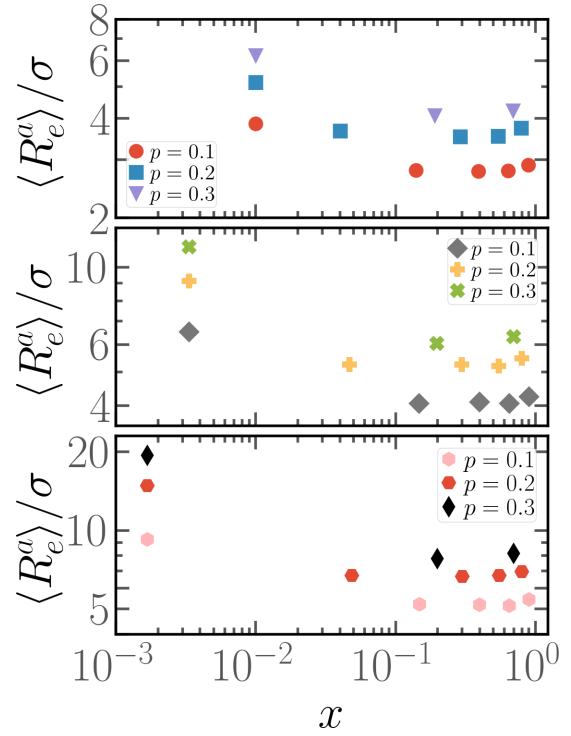

Fig. S10 End-to-end distance of the active section as a function of x for Pe=10, $N = 100$ (a), $N = 300$ (b) and $N = 600$ (c) for different values of p.
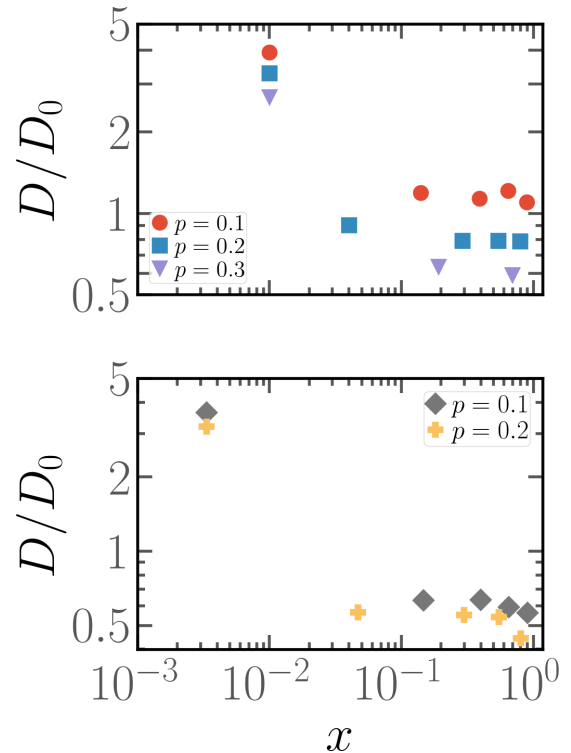

Fig. S11 Estimation of the diffusion coefficient using the stochastic model as a function of x for Pe=10, $N = 100$ (a) and $N = 300$ (b) for different values of p.

for Pe=10, $N =100$ (a) and $N =300$ (b) for different values of p. A comparison with Fig. 8 of the main text shows that the stochastic

model gives reasonable estimates of D/D_0 only for $x \approx 1/N$. On the contrary, for all other values of x, the model overestimates the diffusion coefficient: while the overall decreasing trend of D/D_0 as a function of x is captured, the estimates differ by one order of magnitude or more from the simulation results.
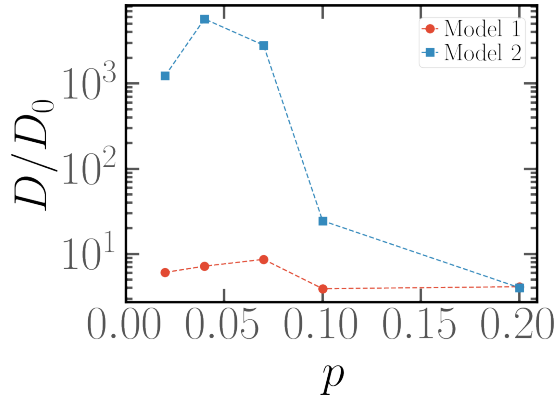

Fig. S12 Estimation of the long time diffusion coefficient D/D_0 using the stochastic model, as a function of p for $x = 1/N$ in "model 1" (red) or "model 2" (blue).

Finally, we consider the predictions from the stochastic model for partially active polymers at very small values of p, $x = 1/N$. In particular, we apply the stochastic model to both "model 1" and "model 2" self-propelled polymers. As reported in the main text, simulation data show that the diffusivity is enhanced by the presence of an active monomer at the head of the chain in "model 2" for $p \leq 0.1$ compared to "model 1". Further, D/D_0 shows a non monotonic behaviour for "model 2".

The predictions of the stochastic model are reported in Fig. S12. We observe that the stochastic model qualitatively reproduces the non-monotonic behaviour in the case of "model 2". However, notably, a slight non-monotonicity is also predicted in the case of "model 1"; as reported in the main text, such behaviour is not observed in the data. Moreover, in both cases, the predicted diffusion coefficient is much larger than the measured value. All in all, these shortcomings show that this very simple stochastic model is not able to recapitulate quantitatively the dynamics of the partially active polymers considered in this work.

7 Multiple active blocks: configurational properties

In this section, we briefly report on the configurational properties of polymers with more than one active block. We choose to report these data as a function of the minimum contour distance between the beginning of the closest active section and the head of the polymer, for the sake of coherence with the rest of the manuscript.

In Fig. S13 we show the mean gyration radius, asphericity and prolateness as a function of the parameter x for polymers of length $N = 500$ with two non-overlapping active blocks at Pe $= 0.1$ (top row), Pe $= 10$. (bottom row) and different values of p. We observe that the shape parameters retain the non-monotonic character also in presence of a second active block; however asphericity and prolateness appear to be more similar, upon varying the fraction of the active monomers p, with respect to the single block

case. On the contrary, the gyration radius as a function of x changes qualitatively in presence of a second active block, losing its non-monotonic character. However, the special nature of arrangements with small x is maintained.

Finally, in Fig. S14 we show the mean gyration radius, asphericity and prolateness as a function of the parameter x for polymers of length $N = 500$ with three non-overlapping active blocks at Pe $= 0.1$ (top row), Pe $= 10$. (bottom row) and different values of p. We can make essentially the same observation as in the two blocks case. All in all, upon increasing the number of blocks, the parameter x appears to become less effective, as highlighted by the more pronounced overlap between the curves, visible in both Figs. S13, S14. Moreover, there is a further symmetry breaking in this representation as, for small values of x, multiple different arrangements share the same value of x, while the same happens at $x \to 1 - p$ only to very few, very similar arrangements.

Notes and references

1 E. Locatelli, V. Bianco, C. Valeriani and P. Malgaretti, *Physical Review Letters*, 2023, **131**, 048101.

2 V. Bianco, E. Locatelli and P. Malgaretti, *Physical Review Letters*, 2018, **121**, 217802.

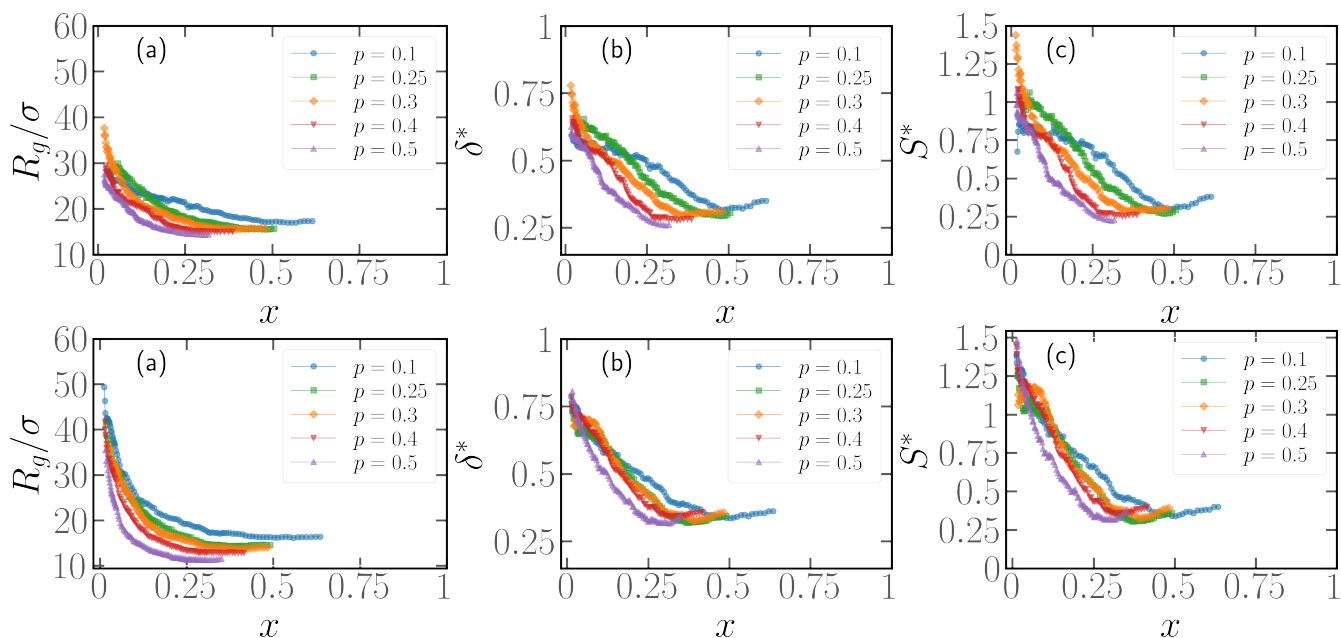3 M. Fazelzadeh, E. Irani, Z. Mokhtari and S. Jabbari-Farouji, *Phys. Rev. E*, 2023, **108**, 024606.

Fig. S13 Mean Gyration Radius (left), asphericity (middle), and prolatness (right) as a function of the parameter x, for polymer chains of $N = 500$ monomers with two non-overlapping active blocks, $Pe = 0.1$ (top row) and $Pe = 10$ (bottom row) and different values of p.
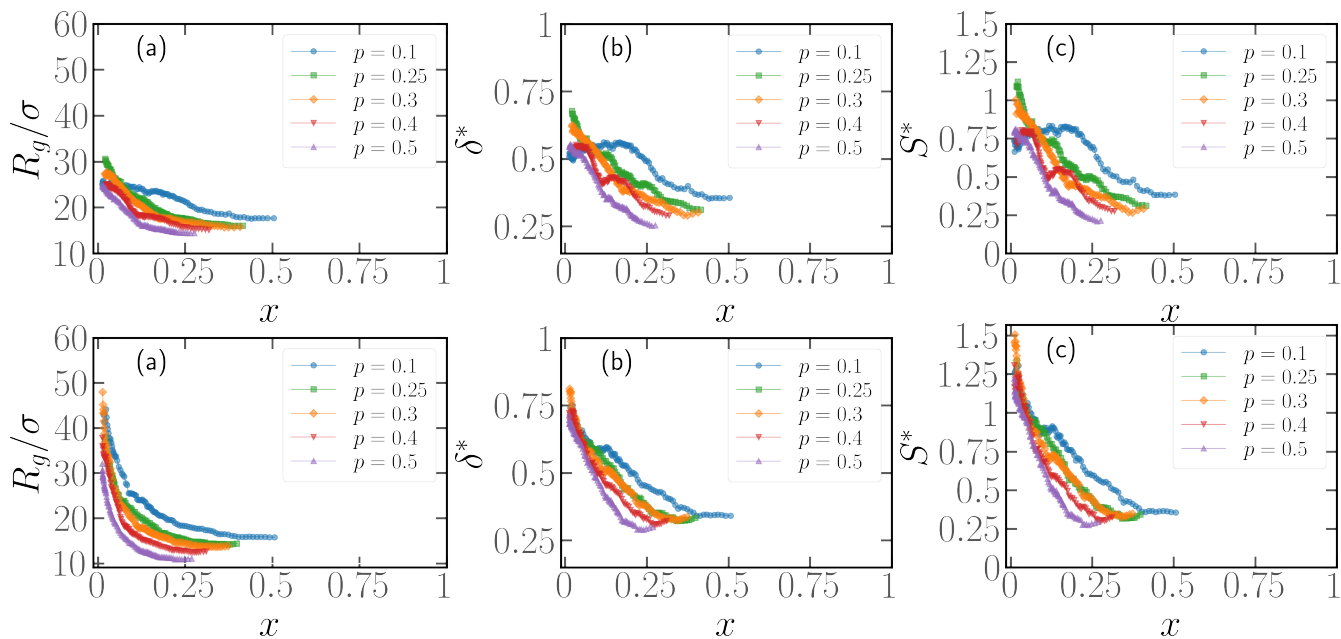

Fig. S14 Mean Gyration Radius (left), asphericity (middle), and prolatness (right) as a function of the parameter x, for polymer chains of $N = 500$ monomers with three non-overlapping active blocks, $Pe = 0.1$ (top row) and $Pe = 10$ (bottom row) and different values of p.